PERGAMON

International Journal of Solids and Structures 38 (2001) 4507–4523

INTERNATIONAL JOURNAL OF SOLIDS and STRUCTURES

www.elsevier.com/locate/ijsolstr

The state of stress induced by the plane frictionless cylindrical contact. I. The case of elastic similarity

Michele Ciavarella [a,*], Paolo Decuzzi [a,b,1]

[a] *Consiglio Nazionale delle Ricerche (CNR–IRIS), Computational Mechanics of Solids (COMES), Str. Crocefisso 2/B, 70125 Bari, Italy*

[b] *Dipartimento di Progettazione e Produzione Industriale, Politecnico di BARI, V. Japigia 182, 70126 Bari, Italy*

Received 13 June 1999; in revised form 29 June 2000

Abstract

The contact problem between cylindrical conformal surfaces, modelling for instance a fastener joint, is studied. A closed form solution is obtained in Part I of the paper for the case of elastic similarity, improving

(i) the solution obtained by Persson (On the Stress Distribution of Cylindrical Elastic Bodies in Contact, Ph.D. dissertation, 1964), which was also limited to identical materials, and

(ii) the results of Noble and Hussain (Int. J. Engng. Sci. 7 (1969) 1149), which were limited to the case of perfect fit of contacting materials.

The variation of the contact area, pressure distribution and maximum sustainable load is given for the complete range of possible dimensionless loading parameter $E_1^*\Delta R/Q$ and first Dundurs' material parameter, α.

Under conditions of initial clearance, the contact area arc, ε, increases with load from zero to a limiting value, $\varepsilon_{\lim}$, which depends only on the material parameter α. Vice versa, under conditions of initial interference, the contact is complete until there is detachment and the contact area starts to decrease with load up to the same limiting value, $\varepsilon_{\lim}$, which is also the only possible value of contact area for neat-fit conditions, under any applied load.

Finally, a complete assessment of the strength of the contact is given for the entire range of working conditions. As expected, the strength of the joint decreases rapidly if the extent of the contact area reduces, and finally tends to the limit predicted by the Hertzian theory when the arc of contact is smaller than about 30°. The optimal conditions for avoiding yielding are reached for a contact arc smaller than the limiting arc $\varepsilon_{\lim}$: this means that it is not possible to reach the optimum from a configuration of initial interference.

Keywords: Elastic similarity; Cylindrical contact; Stress

* Corresponding author. Address: Department of Mechanical Engineering and Applied Mechanics, University of Michigan, Ann Arbor, MI 48109-2125, USA.

E-mail addresses: m.ciavarella@area.ba.cnr.it, decuzzi@engin@umich.edu (M. Ciavarella), p.decuzzi@dppi.poliba.it (P. Decuzzi).

[1] Formely, Visiting Research Investigator at the Department of Mechanical Engineering and Applied Mechanics, University of Michigan, Ann Arbor, MI 48109-2125, USA.

0020-7683/01/$ - see front matter
PII: S0020-7683(00)00289-4

1. Introduction

The plane contact problem for a pin journalled into an infinite plate is an important model for many joints of common use in mechanical applications. For example, pin-loaded attachment lugs are widely employed in aircraft assemblies, particularly when other types of joints, like welding or gluing, are not reliable or feasible. It is obvious that, when the contact area extends only to a small region of the circular domain, the classical Hertzian solution is appropriate, as the bodies can be regarded locally as half-planes, and the circular geometry is well approximated by a parabolic gap function (Johnson, 1985, Sections 4.3 and 5.2). However, in general, the assembly is designed as to spread the load over the largest possible area, rendering the contact significantly "conforming". [2] Under "conformal" conditions, the correct analysis requires influence functions for bodies with circular boundaries; in the case of a concentrated normal force applied at the centre of the pin, the contact is governed by an integro-differential Prandtl's equation of quite cumbersome solution. This was already obtained, by Shtaermann (1949, Section II.7), who also gave an approximate method of solution, but his analysis is obscure and covers only a limited set of cases. An important advance was obtained by Persson (1964) in his Ph.D. thesis, never published in a proper journal, [3] who gave a solution to the limiting case of identical contacting materials; the pressure distribution was found in closed form, whereas the relation load to contact area size was given only in quadrature. Later on, Noble and Hussain (1969) derived a different closed form solution for the case of zero clearance (neat-fit condition) and in the case of elastic similarity of contacting materials, i.e. for Dundurs' parameter $\beta = 0$. Finally, Lin et al. (1997), making use of Persson's analytical procedure, deduced design criteria in the case of identical contacting materials and for a geometry with initial clearance.

The purpose of this present paper is to give a completely closed form solution to the contact problem, for the general case of elastically similar materials in frictionless contact. Starting from the solution of Persson (1964), a closed form formula is obtained for both pressure distribution and the load to contact area size relation in the general case $\beta = 0$ and with arbitrary initial gap or interference.

2. Formulation – Persson's results

The lug problem is idealized as a cylindrical bolt, of radius R_1, journalled in an infinite plate with a hole of radius R_2 (Fig. 1). Both the pin and the plate are made of isotropic elastic materials. The following nondimensional quantities are considered by Persson (1964):

$$\begin{aligned} &E_1^*\Delta R/Q, \text{ (load parameter)},\\ &\eta = E_1^*/E_2^*, \text{ (first material parameter)},\\ &\lambda = \left(1-\nu_1^*\right) - \eta\left(1-\nu_2^*\right), \text{ (second material parameter)}, \end{aligned} \tag{1}$$

where suffixes 1 and 2 refer to the pin and the plate, respectively; $\Delta R = R_2 - R_1$ represents the radial clearance of the joint, Q is the external load, applied at the center of the pin; E_i^* and ν_i^* are the modified Young's modulus and Poisson's ratio:

[2] More precise design criteria will be given later, where it will be shown that the minimum of von Mises criteria is reached for a particular contact arc, whereas for the minimum tension the contact should be designed with interference.

[3] However, retriving the original Ph.D. thesis as interlibrary loan was not difficult for us, by sending a request to "The Library of the Chalmers University of Technology, S-41298 Gothenburg, Sweden". Web site http://www.lib.chalmers.se/eindex.html

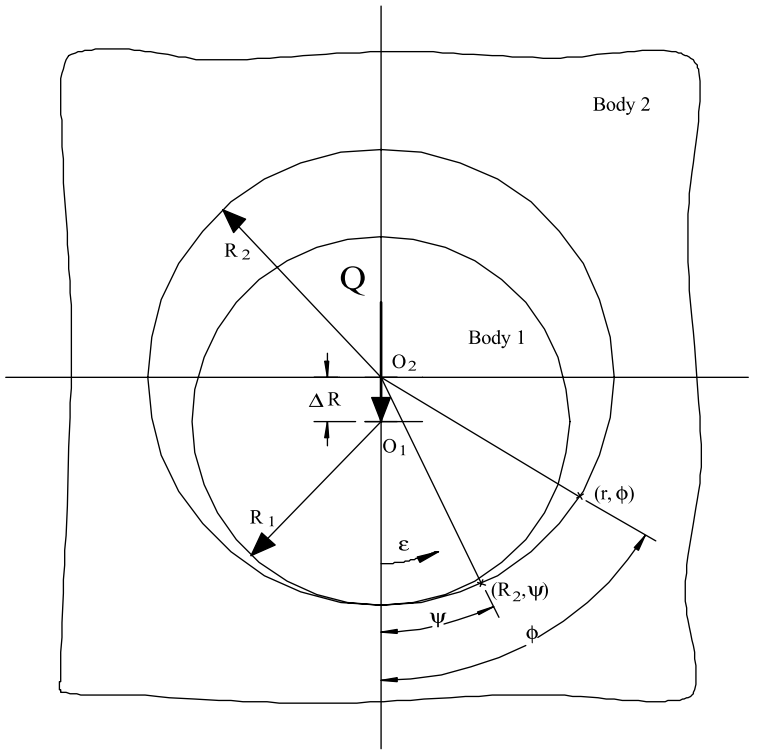

Fig. 1. Geometry and symbols used.

$$E_i^* = \frac{E_i}{1-\nu_i^2} \quad \text{(plane strain)}, \qquad E_i^* = E_i \quad \text{(plane stress)},$$
$$\nu_i^* = \frac{\nu_i}{1-\nu_i} \quad \text{(plane strain)}, \qquad \nu_i^* = \nu_i \quad \text{(plane stress)}. \tag{2}$$

Following Persson (1964), the contact condition at the hole surface are determined in terms of radial displacements, which are then expressed as functions of an unknown contact pressure (Appendix A), employing classical formulae appropriate for cylindrical bodies. After some algebra, finally he derives the following singular integro-differential governing equation:

$$\int_{-b}^{+b} q'(t)\frac{\mathrm{d}t}{t-y} + \frac{\lambda\pi}{1+\eta}\frac{q(y)}{1+y^2} = -\frac{4k}{\pi(1+y^2)^2} + \frac{B}{1+y^2},$$
$$B = \frac{2k}{\pi} - \frac{2\eta}{1+\eta}\int_{-b}^{+b} q(t)\frac{\mathrm{d}t}{1+t^2} - \frac{\pi}{(1+\eta)}\frac{E_1^*\Delta R}{Q}, \tag{3}$$

which, together with the following closure condition given by overall equilibrium

$$\int_{-b}^{+b} q(t)\frac{1-t^2}{(1+t^2)^2}\mathrm{d}t = \frac{1}{2} \tag{4}$$

is solved for the dimensionless contact pressure $q(y) = R_2 p(y)/Q$ and for the semi-angle of contact ε. The auxiliary variables b, t, y and k are defined as

$$y=\tan(\phi/2),\qquad t=\tan(\psi/2),\qquad b=\tan(\varepsilon/2), \tag{5}$$

$$k=\frac{\pi}{2}\frac{2(1+\eta)-\lambda}{1+\eta} \tag{6}$$

with ε being the semi-angle of contact, and ψ and ϕ as in Fig. 1.

In the case of identical material in contact ($\eta=1;\lambda=0$), Persson gives a complete solution. The main equations. (3) in this case reduces to

$$\int_{-b}^{+b} q'(t)\frac{\mathrm{d}t}{t-y}=-\frac{4}{(1+y^2)^2}+\frac{B}{1+y^2},\quad B=2-\int_{-b}^{+b}\frac{q(t)}{1+t^2}\mathrm{d}t-\frac{\pi}{2}\frac{E^*\Delta R}{Q}, \tag{7}$$

together with the closure condition (4). This equation can be inverted analytically for $q'(t)$ and then integrating with respect to t, gives eventually a closed form solution

$$\frac{Rp(y)}{Q}=\frac{2}{\pi\sqrt{b^2+1}}\frac{\sqrt{b^2-y^2}}{1+y^2}+\frac{1}{2\pi b^2(1+b^2)}\log\frac{\sqrt{b^2+1}+\sqrt{b^2-y^2}}{\sqrt{b^2+1}-\sqrt{b^2-y^2}}, \tag{8}$$

and the semi-angle of contact, ε, is given only in quadrature by

$$\frac{E^*\Delta R}{Q}=\frac{2}{\pi}\frac{1-b^2}{b^2}-\frac{I_b}{\pi^2 b^2(1+b^2)}, \tag{9}$$

with the following integral I_b:

$$I_b=\int_{-b}^{b}\log\frac{\sqrt{b^2+1}+\sqrt{b^2-t^2}}{\sqrt{b^2+1}-\sqrt{b^2-t^2}}\frac{\mathrm{d}t}{1+t^2}, \tag{10}$$

numerically evaluated by Persson. Thus, the best way to solve Eq. (9) is by first fixing b, followed by evaluating numerically the integral I_b and by substituting back to find the corresponding load parameter.

3. Extension for $\alpha\neq 0$

Dundurs's material parameters α and β are defined as (Dundurs, 1969, 1975)

$$\begin{aligned}\alpha&=\frac{(\mu_2/\mu_1)(\kappa_1+1)-(\kappa_2+1)}{\mu_2/\mu_1(\kappa_1+1)+(\kappa_2+1)}=\frac{((\kappa_1+1)/\mu_1)-((\kappa_2+1)/\mu_2)}{((\kappa_1+1)/\mu_1)+((\kappa_2+1)/\mu_2)},\\ \beta&=\frac{(\mu_2/\mu_1)(\kappa_1-1)-(\kappa_2-1)}{(\mu_2/\mu_1)(\kappa_1+1)+(\kappa_2+1)}=\frac{((\kappa_1-1)/\mu_1)-((\kappa_2-1)/\mu_2)}{((\kappa_1+1)/\mu_1)+((\kappa_2+1)/\mu_2)},\end{aligned} \tag{11}$$

where $\mu_i=E_i/[2(1+\nu_i)]$ is the shear modulus and κ_i is Kolosoff's constant:

$$\kappa_i=\frac{3-\nu_i}{1+\nu_i}\quad\text{(plane stress)},\qquad \kappa_i=3-4\nu_i\quad\text{(plane strain)}. \tag{12}$$

For identical materials the two Dundurs' parameters are zero. By substituting Eq. (1) into Eq. (11), the following relations with Persson's parameters hold:

$$\alpha=\frac{1-\eta}{1+\eta},\qquad \beta=\frac{1}{2}\frac{\lambda}{1+\eta},\qquad \eta=\frac{1-\alpha}{1+\alpha},\qquad \lambda=\frac{4\beta}{1+\alpha},\quad k=\pi(1-\beta), \tag{13}$$

where η, λ and k are defined as in Section 1. Thus,

$$\frac{\lambda\pi}{1+\eta}=2\beta\pi,\qquad \frac{2\eta}{1+\eta}=(1-\alpha),\qquad \frac{2k}{\pi}=2(1-\beta),\qquad \frac{\pi}{1+\eta}=\frac{\pi}{2}(1+\alpha). \tag{14}$$

Using Dundurs' parameters, the governing equations given by Persson (Section 2) take the following form:

$$\int_{-b}^{+b}\frac{q'(t)}{t-y}\mathrm{d}t+\frac{2\pi\beta}{1+y^2}q(y)=-\frac{4(1-\beta)}{(1+y^2)^2}+\frac{B}{1+y^2}, \tag{15}$$

where

$$B=2(1-\beta)-(1-\alpha)\int_{-b}^{+b}q(t)\frac{\mathrm{d}t}{1+t^2}-\frac{\pi}{2}(1+\alpha)\frac{E_1^*\Delta R}{Q} \tag{16}$$

with the closure condition (4).

Thus, if $\beta=0$, the previous equations simplify to

$$\int_{-b}^{+b}\frac{q'(t)}{t-y}\mathrm{d}t=-\frac{4}{(1+y^2)^2}+\frac{B}{1+y^2}, \tag{17}$$

$$B=2-(1-\alpha)\int_{-b}^{+b}q(t)\frac{\mathrm{d}t}{1+t^2}-\frac{\pi}{2}(1+\alpha)\frac{E_1^*\Delta R}{Q}. \tag{18}$$

By comparison with Persson's equations in the case of identical materials in contact (Eq. (7)), it is clear that the parameter α affects only the relationship between the contact angle ε and the load parameter $E_1^*\Delta R/Q$. In particular, the dimensionless pressure distribution $q(y)$ has the same mathematical form of that given by Persson. In fact, following Persson's procedure and inverting Eq. (18) for $q'(t)$, it follows that

$$q(y)=\frac{2\sqrt{b^2-y^2}}{\pi\sqrt{b^2+1}(1+y^2)}+\frac{1}{\pi}\left(1-\frac{B}{2}\right)\log\frac{\sqrt{b^2+1}+\sqrt{b^2-y^2}}{\sqrt{b^2+1}-\sqrt{b^2-y^2}}. \tag{19}$$

The constant B is evaluated by substituting Eq. (19) in Eq. (??), and integrating with respect to t, Persson obtains

$$B=\frac{2b^4+2b^2-1}{b^2(b^2+1)}. \tag{20}$$

Now, substituting this into Eq. (19), the dimensionless pressure distribution as in Persson's case (8) is obtained. The difference with Persson's treatment is in the relation between the contact area and loading parameter (18) which, with Eq. (20) becomes

$$\frac{\pi}{2}(1+\alpha)\frac{E_1^*\Delta R}{Q}=2-\frac{2b^4+2b^2-1}{b^2(b^2+1)}-(1-\alpha)\int_{-b}^{+b}q(t)\frac{\mathrm{d}t}{1+t^2}. \tag{21}$$

In order to solve the integral in the right-hand side, Persson (1964, Appendix 6.6) obtains

$$\int_{-b}^{+b}q(t)\frac{\mathrm{d}t}{1+t^2}=\frac{1}{2\pi}\frac{I_b}{b^2(b^2+1)}+\frac{b^2}{(b^2+1)}, \tag{22}$$

where the integral I_b is given again by Eq. (10).

I_b is here evaluated analytically and differently from Persson's, with the change of variables (5), obtaining

$$I_b=\int_{-\varepsilon}^{+\varepsilon}\log\left[\frac{\cos(\psi/2)+\sqrt{\cos^2(\psi/2)-\cos^2(\varepsilon/2)}}{\cos(\varepsilon/2)}\right]\mathrm{d}\psi, \tag{23}$$

which is analytically integrable by making use of the results given in the appendix of Noble and Hussain (1969), obtaining

$$I_b = -2\pi \log\left[\cos\left(\varepsilon/2\right)\right] = \pi \log\left[1 + b^2\right]. \tag{24}$$

Therefore, the loading parameter–contact angle relation is given by

$$\frac{E_1^* \Delta R}{Q} = \frac{(\alpha - 1)(\log\left[b^2 + 1\right] + 2b^4) + 2}{\pi(1 + \alpha)(b^2 + 1)b^2}, \tag{25}$$

whereas the pressure distribution is the same as in Persson's case of identical materials (8).

It is fairly clear that (i) the pressure distribution (8) is independent of Dundurs' parameter α, (ii) only relationship (25) between the contact angle ε and the load parameter is affected by the first Dundurs' parameter.

In addition, the maximum dimensionless contact pressure ($y = 0$) is given, from Eq. (8) by

$$q_0 = \frac{2b}{\pi\sqrt{b^2 + 1}} + \frac{\log\left[\sqrt{b^2 + 1} + b\right]}{\pi b^2 (1 + b^2)}, \tag{26}$$

which is formally identical to those given by Persson but takes obviously different values at fixed load parameters and α. The maximum of the dimensionless pressure has an absolute minimum, as it is seen in Fig. 3, at $\varepsilon = 105.573°$, with $q_0 = 0.580093$.

4. Special cases

In the following, three special cases are studied in some details, namely (i) the limiting case of Hertzian contact ($b \to 0$), (ii) the neat fit or infinite load condition ($E_1^* \Delta R/Q = 0$) and (iii) the complete contact case ($b \to \infty$).

4.1. Hertzian contact

When the applied load is small or the radial clearance is large, the Hertzian contact problem is approached. Imposing that the contact patch semi-width is given by $R_2\varepsilon$ and generalizing, consequently, the classical formulae (Johnson, 1985, Sections 4.3 and 5.2; Hills et al., 1993, Section 2.3), the following relations hold for the dimensionless pressure distribution:

$$q(\psi) = -q_0\sqrt{1 - (\psi/\varepsilon)^2}, \quad q_0 = \frac{p_0}{Q/R_2} = \frac{2}{\pi\varepsilon} \approx \frac{1}{\pi b}, \tag{27}$$

and for the contact angle

$$\varepsilon^2 = \frac{2QA}{\pi R_2^2 k} = \frac{8}{\pi(\alpha + 1)} \frac{Q}{E_1^* \Delta R}, \tag{28}$$

where

$$\begin{aligned} A &= \frac{\kappa_1 + 1}{4\mu_1} + \frac{\kappa_2 + 1}{4\mu_2} = \frac{4}{(\alpha + 1)E_1^*}, \\ k &= \frac{1}{R_1} - \frac{1}{R_2} \approx \frac{\Delta R}{R_2^2}. \end{aligned} \tag{29}$$

The pressure distribution given in Eq. (8) tends to Eq. (27) as b approaches zero. In fact, expanding the logarithmic term of Eq. (8) in powers of $\sqrt{(b^2-y^2)/(b^2+1)}$, follows that

$$\log\left[\frac{\sqrt{b^2+1}+\sqrt{b^2-y^2}}{\sqrt{b^2+1}-\sqrt{b^2-y^2}}\right]=\log\left[\frac{c+z}{c-z}\right]=2\sum_{1,2}^{\infty}\left(\frac{z}{c}\right)^n=2\sum_{1,2}^{\infty}\left(\sqrt{\frac{b^2-y^2}{b^2+1}}\right)^n. \tag{30}$$

Hence, evaluating the limit for $b\to 0$

$$\begin{aligned} q(y)&=\lim_{b\to 0}\left\{\frac{2}{\pi\sqrt{b^2+1}}\frac{\sqrt{b^2-y^2}}{1+y^2}+\frac{1}{\pi b^2(1+b^2)}\sum_{1,2}^{\infty}\left(\sqrt{\frac{b^2-y^2}{b^2+1}}\right)^n\right\},\\ &=\lim_{b\to 0}\frac{2}{\pi\sqrt{b^2+1}}\left\{\frac{\sqrt{b^2-y^2}}{1+y^2}+\frac{1}{2b^2}\sum_{1,2}^{\infty}\frac{(b^2-y^2)^{n/2}}{(b^2+1)^{(n+1)/2}}\right\}=\frac{\sqrt{b^2-y^2}}{\pi b^2}, \end{aligned} \tag{31}$$

as only the term corresponding to $n=1$ is non-zero

$$\lim_{b\to 0}\frac{1}{(b^2+1)}\frac{\sqrt{b^2-y^2}}{2b^2}=\frac{\sqrt{b^2-y^2}}{2b^2}, \tag{32}$$

$$\lim_{b\to 0}\frac{1}{2b^2}\sum_{3,2}^{\infty}\frac{(b^2-y^2)^{n/2}}{(b^2+1)^{(n+1)/2}}=\lim_{b\to 0}\frac{1}{2}\sum_{3,2}^{\infty}\frac{\left(\frac{b^2-y^2}{b^{4/n}}\right)^{n/2}}{(b^2+1)^{(n+1)/2}}=0,\quad 4/n<2.$$

By using Eq. (5) in Eq. (31), the Hertzian result is obtained (Eq. (27)). For the load parameter, the Hertzian asymptotic value is given by

$$\left[\frac{E_1^*\Delta R}{Q}\right]_{\mathrm{H}}=\lim_{b\to 0}\frac{(\alpha-1)(\log[b^2+1]+2b^4)+2}{\pi(\alpha+1)b^2(b^2+1)}=\frac{2}{\pi(\alpha+1)b^2}, \tag{33}$$

which after simple algebraic manipulations and considering that $b=\tan(\varepsilon/2)\simeq\varepsilon/2$, gives Eq. (28).

4.2. Neat-fit or infinite load condition

The neat-fit condition is determined for a zero initial radial clearance ΔR or an infinite applied load Q. When this limiting condition is approached, the load parameter assumes a constant value ($E_1^*\Delta R/Q=0$), independently of how large is Q, at which corresponds a fixed contact angle $\varepsilon_{\lim}$ depending only on the material parameter α. Consequently, the neat-fit case ($\Delta R=0$) results in a border condition between the advancing contact clearance fit ($\Delta R>0$) and the receding interference fit ($\Delta R<0$). This is in perfect agreement with the statement reported by Gladwell (1980, Section 4.10). In addition, it is fairly clear that, under such limiting condition, the contact pressure, distributed over a constant area, increases linearly with the applied load and so does the severity of the internal stress field.

The limiting angle is evaluated by solving the implicit equation (25), that is

$$\log\left[b^2+1\right]+2b^4=-\frac{2}{(\alpha-1)}, \tag{34}$$

which exactly coincides with the result given by Noble and Hussain (1969), using Eq. (5) and the Noble and Hussain material parameter. In Fig. 5, the limiting contact angle is illustrated as a function of Dundurs's parameter α, and some results are listed in Table 1, which can be readily compared with those given by Noble and Hussain (1969).

Table 1
Contact angles for different values of Dundurs' parameter in the neat fit condition ($\Delta R = 0$)

α	b	ε°
−1.0	0.7324	72.44
−0.8	0.7573	74.27
−0.6	0.7871	76.42
−0.4	0.8218	78.83
−0.2	0.8631	81.59
0	**0.9136**	**84.83**
+0.2	0.9779	88.72
+0.4	1.0652	93.62
+0.6	1.1973	100.26
+0.8	1.4510	110.85

4.3. Complete contact

For interference fit condition, there are infinite values of the load parameter corresponding to complete contact ($\varepsilon = 180°$), and these are all the values smaller than the critical load parameter $E_1^*\Delta R/Q$ at the onset of separation. These limiting values are readily determined by evaluating the limit of $E_1^*\Delta R/Q$ as b tends to infinity, thus by Eq. (25),

$$\left[\frac{E_1^*\Delta R}{Q}\right]_{\lim} = \lim_{b\to\infty} \frac{(\alpha-1)(\log[b^2+1]+2b^4)+2}{\pi(\alpha+1)b^2(b^2+1)} = \frac{2}{\pi}\frac{\alpha-1}{\alpha+1}, \tag{35}$$

which is identical to the result given, only for plane stress assumption, by Ghosh et al. (1981). Some numerical results are given in Table 2:

In addition, for complete contact, the pressure distribution is given by

$$q(y) = \frac{2}{\pi}\frac{1}{1+y^2}, \qquad q(0) = \frac{2}{\pi}. \tag{36}$$

Relation (36) is simply achieved by evaluating the limit of $q(y)$ as b tends to infinity and by employing the series expansion of the logarithmic term as in Eq. (30).

Table 2
Limiting values of the load parameter at the onset of separation

α	$E_1^*\Delta R/Q$
−1.0	$-\infty$
−0.8	−5.72958
−0.6	−2.54648
−0.4	−1.48545
−0.2	−0.95493
0	$\mathbf{-2/\pi}$
+0.2	−0.424413
+0.4	−0.272837
+0.6	−0.159155
+0.8	−0.0707355
+1.0	0.0

5. Internal stress field

The stress field in the infinite plate is given by Persson (1964, Section 3.3) as

$$\begin{aligned} -\tilde{\sigma}_{rr}+\tilde{\sigma}_{\phi\phi} &= \frac{1}{\pi}\int_{-\varepsilon}^{+\varepsilon} q(\psi)\mathrm{d}\psi + 2\int_{-\varepsilon}^{+\varepsilon} q(\psi)L_1\,\mathrm{d}\psi + \frac{3-v_2^*}{2\pi\rho}\cos\phi, \\ \tilde{\sigma}_{rr} &= \frac{\rho-1}{2\pi\rho}\int_{-\varepsilon}^{+\varepsilon} q(\psi)\mathrm{d}\psi + \int_{-\varepsilon}^{+\varepsilon} q(\psi)L_2\,\mathrm{d}\psi + \frac{3-v_2^*}{4\pi}\frac{\rho^2-1}{\rho^3}\cos\phi, \\ \tilde{\sigma}_{r\phi} &= \int_{-\varepsilon}^{+\varepsilon} q(\psi)L_3\,\mathrm{d}\psi + \frac{3-v_2^*}{4\pi}\frac{\rho^2-1}{\rho^3}\sin\phi, \end{aligned} \tag{37}$$

where $\rho = r/R_2$, $\tilde{\sigma}_{ij} = \sigma_{ij}/(Q/R_2)$ and influence functions L_i are

$$\begin{aligned} L_1 &= \frac{1}{2\pi}\frac{(1-\rho^2)}{(\rho^2-2\rho\cos\theta+1)}, \\ L_2 &= \frac{1}{2\pi}\frac{(1-\rho^2)^2}{\rho}\frac{(\cos\theta-\rho)}{(\rho^2-2\rho\cos\theta+1)^2}, \quad \theta=\psi-\phi, \\ L_3 &= \frac{1}{2\pi}\frac{(1-\rho^2)^2}{\rho}\frac{\sin\theta}{(\rho^2-2\rho\cos\theta+1)^2}. \end{aligned} \tag{38}$$

As ρ approaches unity, the L_i functions become singular. However, stresses on the hole surface ($\rho = 1$) are determined directly as (Persson, 1964, Section 2.33)

$$\tilde{\sigma}_{\phi\phi}(\psi)-\tilde{\sigma}_{rr}(\psi) = \frac{3-v_2^*}{2\pi}\cos\psi + \frac{1}{\pi}\int_{-\varepsilon}^{+\varepsilon} q(\psi)\mathrm{d}\psi, \qquad \tilde{\sigma}_{rr}(\psi) = -q(\psi), \qquad \tilde{\sigma}_{r\phi}(\psi) = 0, \tag{39}$$

thus, avoiding, the singularity. Moreover, from Eqs. (5), (22) and (24), it follows that

$$\int_{-\varepsilon}^{+\varepsilon} q(\psi)\mathrm{d}\psi = 2\int_{-b}^{+b}\frac{q(t)}{(1+t^2)}\mathrm{d}t = \frac{\log[b^2+1]+2b^4}{b^2(b^2+1)}. \tag{40}$$

Thus, substituting Eq. (40) into Eq. (39), we obtain a closed form result

$$\tilde{\sigma}_{\phi\phi}(\psi) = -q(\psi) + \frac{3-v_2^*}{2\pi}\cos\psi + \frac{\log[b^2+1]+2b^4}{\pi b^2(b^2+1)}. \tag{41}$$

In general, integrals in Eq. (37) are evaluated numerically by means of standard Gauss–Chebyshev quadrature (Davis and Rabinowitz, 1984, Section 3.27).

6. Strength of the contact

In Fig. 2, the normalized pressure distribution (Eq. (8)) is illustrated as a function of the angular abscissa ψ and for different contact angles ε. As the contact angle increases, the pressure distribution shape diverges from the typical semi-elliptical Hertzian distribution. It is important to notice that for intermediate contact angles, the pressure distribution is more uniform than for the limiting cases (Hertzian and complete contact). In the Hertzian case, the maximum tends to infinity (Eq. (27)) carrying to a very localized distribution. Vice versa, for complete contact the pressure is very low in the neighborhood of $\psi = 180$. This particular behavior is emphasized in Fig. 3, where the maximum pressure distribution (Eq. (26)) is plotted

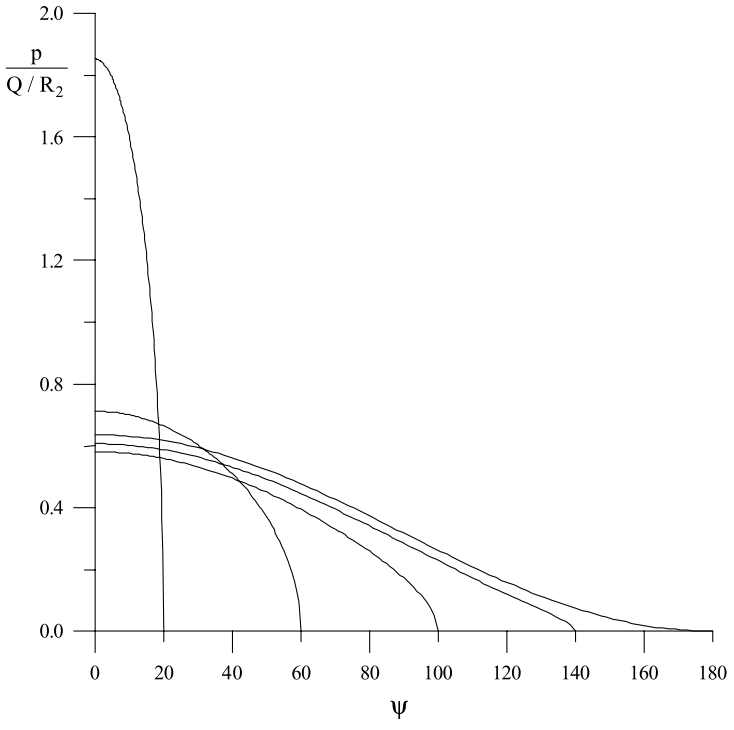

Fig. 2. Normalized pressure distribution over the contact patch, for different values of the contact angle.

against the angular parameter b. Independently on the choice of materials, a minimum appears at $\psi = 105.57°$, and the Hertzian limit is approached (Eq. (27)) for small values of b, whilst the limit is given by $2/\pi$ (Eq. (36)) for complete contact.

The relationship between the load parameter $E_1^*\Delta R/Q$, b and Dundurs' parameter α (Eq. (25)) is illustrated on Fig. 4. For small values of b, the load parameter tends to the Hertzian limit (Eq. (33)), which is represented by a straight line in a log–log diagram, whereas for b tending to infinity, complete contact is approached (Eq. (35)).

For initial gap, the contact starts in the Hertzian regime and at infinite load $\varepsilon_{\lim}$ is reached. For initial interference, the contact stays complete until a certain limiting load has been reached (Eq. (35)), after which separation occurs; at infinitely high load $\varepsilon_{\lim}$ is reached again. For the neat-fit condition ($E_1^*\Delta R/Q = 0$), the only possible contact angle is $\varepsilon_{\lim}$, for which the problem becomes linear and no more contact angle variation with load is registered. At the neat-fit condition the curves present a vertical tangent which indicates also the limiting angle. The influence of the material parameter α is also illustrated too, with parametric curves for different values of Dundurs' parameter, namely $\alpha = -1.0$ div. $+ 1.0$ with a step of 0.2. The parametric curves have a common intersection point at $\varepsilon_i = 72.35°$ ($b = 0.731$) and $\left[E_1^*\Delta R/Q\right]_i = 0.388$ which is simply determined analytically by solving the equation $E_1^*\Delta R/Q(b,\alpha_1) = E_1^*\Delta R/Q(b,\alpha_2)$ for b. This point, which happens to be in the clearance fit region, separates the diagram in two different zones: in the interference fit area and in a small part of the clearance fit close to the neat fit condition, increasing α at fixed b gives an increase of the loading parameter, whilst for $E_1^*\Delta R/Q > \left[E_1^*\Delta R/Q\right]_i$ the behavior is perfectly inverted.

The limiting contact angles $\varepsilon_{\lim}$ are plotted on Fig. 5 as a function of the Dundurs' parameter α (Eq. (34)). As previously remarked, $\varepsilon_{\lim}$ increases with α growing from -1 (perfectly rigid disk) up to $+1$

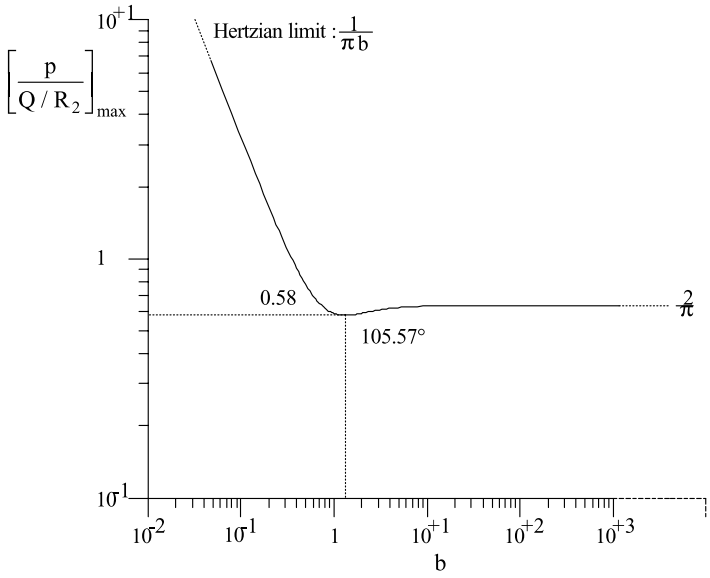

Fig. 3. Maximum of the normalized pressure distribution as a function of the angular parameter b.

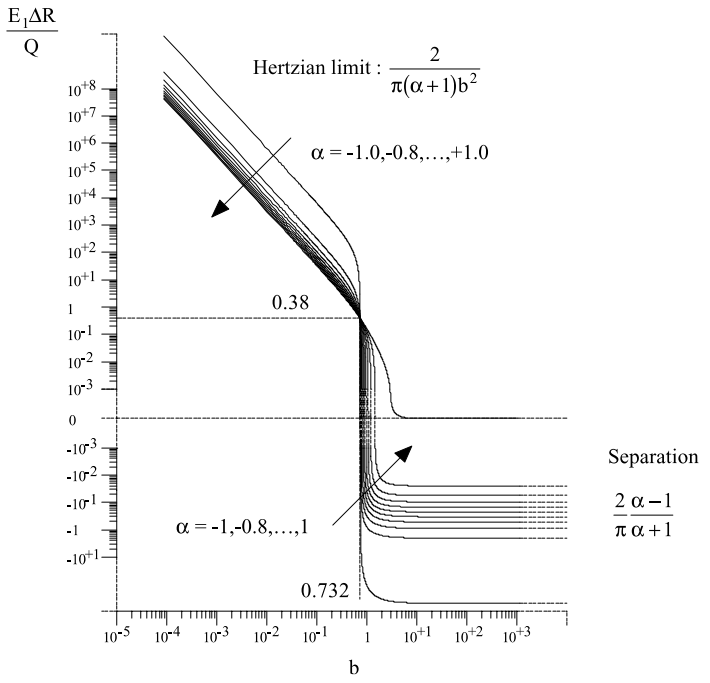

Fig. 4. The relationship between the design parameter $E_1^*\Delta R/Q$ and the angular parameter b, for different values of Dundurs' parameter $\alpha = -1, -0.8, \ldots, 1$.

(perfectly rigid plate). In particular, for $\alpha = +1$, the limiting angle coincides with complete contact; thus, only for the couple of materials, it is possible to reach a complete contact starting with positive clearance

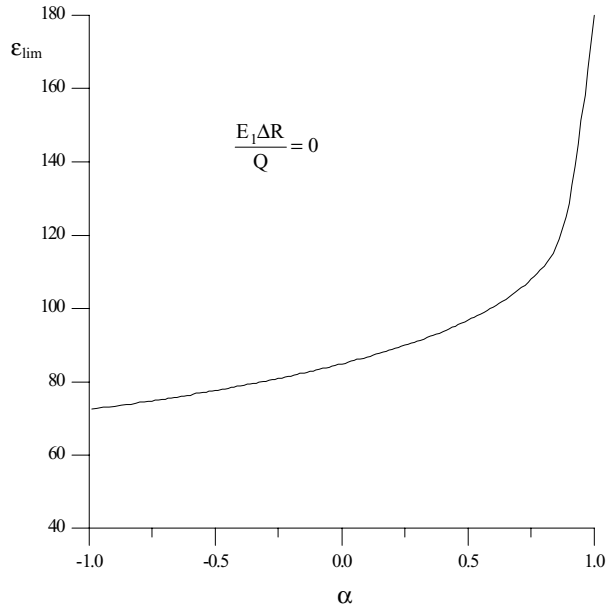

Fig. 5. The limiting contact angle for neat-fit condition as a function of Dundurs' parameter α.

and steadily increasing steadily the applied load. Moreover, starting with interference, a complete contact is always registered for any applied load.

In Fig. 6 the analytically determined hoop stresses on the hole surface (Eq. (41)), normalized with respect to the applied load Q and the hole radius R_2, are illustrated as a function of angular abscissa ψ, for different contact angles and for $v_2 = 0.3$. As the contact angle is increased, a more uniform distribution of the hoop stresses appears and the shape of the curves changes strongly. Three characteristic points are remarkable, namely $\psi = 0.0$, $\psi = \varepsilon$ and $\psi = 180°$. The values of the hoop stresses gives rise, for a material having a maximum admissible tensile stress σ_{adm}, to a limiting load plotted on Fig. 7 for different values of Poisson' ratio of the plate.

In Fig. 8, contour plots of the normalized von Mises parameter are presented for different contact angles, namely $\varepsilon = 30°$, 70°, 110° and 150°. The maximum is always at $\psi = 0°$, and it moves progressively toward the surface as the contact angle is increased.

Finally, the maximum sustainable load according to von Mises' criterion, is illustrated in Fig. 9, for different Poisson's ratio as a function of the angular parameter b. For small contact angles, the curves tend to the Hertzian limit $3.1\pi b$. This result derives from the relation $p_0/\sqrt{J_2} = 3.1$ given by Hills et al. (1993) and Eq. (27). On the hole surface, the dimensionless yielding parameter is determined analytically by substituting in the classical von Mises formula for plane strain,

$$\left[\frac{\sqrt{J_2}}{Q/R_2}\right]_{max} = \sqrt{\frac{1}{3}\left[(v_2^2 - v_2 + 1)\tilde{\sigma}_{rr}^2 + (2v_2^2 - 2v_2 - 1)\tilde{\sigma}_{rr}\tilde{\sigma}_{\phi\phi} + (v_2^2 - v_2 + 1)\tilde{\sigma}_{\phi\phi}^2\right]} \tag{42}$$

the results given in Eqs. (39) and (41). For high contact angles, this tends to a limit:

$$\lim_{b\to\infty}\left[\frac{\sqrt{J_2}}{Q/R_2}\right]_{max} = \sqrt{\frac{2}{3\pi}\left(\frac{2}{\pi}(v_2^2 - v_2 + 1)\left[1 + \frac{(3 - v_2)^2}{16}\right] - (2v_2^2 - 2v_2 - 1)\frac{3 - v_2}{2\pi}\right)}. \tag{43}$$

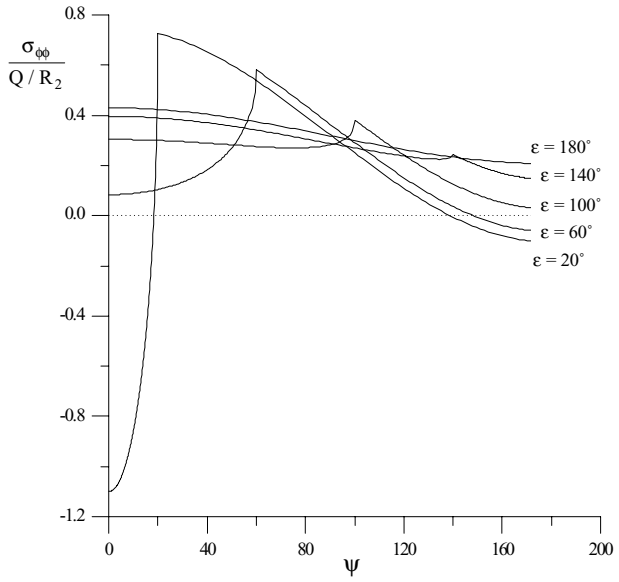

Fig. 6. Dimensionless hoop stresses over the hole surface for different contact angles and with Poisson's ratio $v_2 = 0.3$.

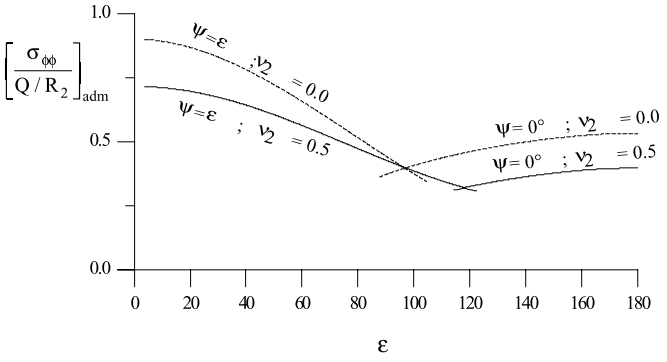

Fig. 7. The variation of the maximum admissible hoop stresses with Poisson's ratio v_2 and the contact angle ε.

The maximum is influenced by Poisson's ratio, and increases with it. In addition, maxima are located in the clearance-fit region (the straight vertical dotted lines separates the region of clearance fit from that of neat fit). For small contact angles, the maxima are subsurface controlled (dotted lines), whereas solid lines are referred to surface controlled maxima. The case with additional initial interference in the contact could be easily studied, as the maximum will be certainly on surface, by adding the contribution due to the uniform term.

7. Conclusions

A completely closed form solution to the problem of cylindrical bodies in contact has been given, for the general case of elastically similar materials in frictionless contact, which has applications as a model for many joints used in mechanical components. Results are given for the complete range of variation of the first Dundurs' material parameter, α. It is found that the effect of α is strong on the load to contact area size

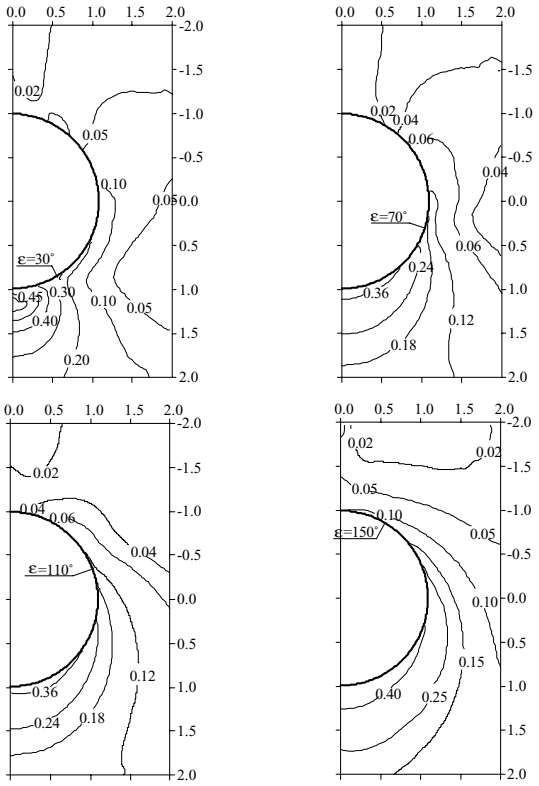

Fig. 8. Contour plots of the von Mises dimensionless parameter $\sqrt{J_2}/(Q/R_2)$ for different contact angles and with $\nu_2 = 0.3$ (plane strain).

relation, and this can be seen in particular very clearly on the limiting angle of contact, i.e. the angle of contact at very high loads (or the only possible angle of contact with neat-fit conditions) which varies from about 70–180°.

On the other hand, the pressure distribution depends *only* on the angle of contact, which in turn depends on the loading conditions (the parameter $E_1^* \Delta R/Q$, below) and α. In other words, the pressure has the same functional form as in the Persson's identical materials case, it is only the relation load–area to have a more general dependence. As a consequence, the strength of the contact depends only on one parameter, and therefore the results already obtained by Lin et al. (1997), which were limited for $\varepsilon < 80$ are here integrated giving general design criteria for any ε and combination of materials provided by $\beta = 0$. In particular, the optimal condition with respect to von Mises yielding parameter is reached for contact arc angles just smaller than ε_{lim}.

In Part II of this paper, a computational algorithm is presented, which can be easily implemented in symbolic mathematical softwares, to estimate the pressure distribution, stress field and maximum yielding parameter as a function of the input data.

Appendix A

In his Ph.D. thesis, Persson (1964) demonstrates that, in the two limiting cases of a rigid plate or a rigid pin, the difference $(\tilde{u}_2 - \tilde{u}_1)$ between the radial displacements at the contact region are independent of the

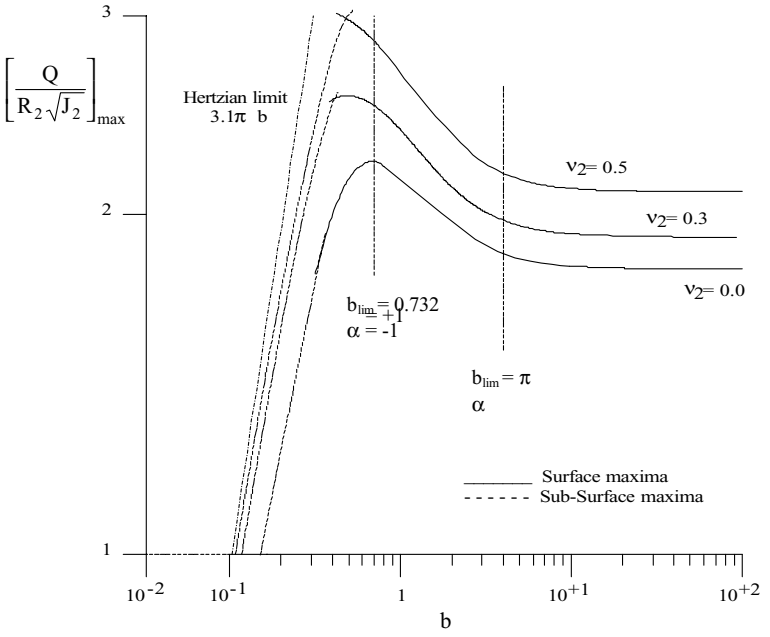

Fig. 9. The maximum sustainable load as a function of the angular parameter b, for different Poisson's ratios (plane strain).

tangential displacements $\tilde{v}$, if second-order terms are neglected. Assuming that the same holds true in the general case of two elastic bodies (Fig. 10), Persson shows that

$$\tilde{u}_2 - \tilde{u}_1 = \delta\cos\phi - (R_2 - R_1)(1 - \cos\phi), \tag{A.1}$$

where $\delta = \tilde{u}_{02} - \tilde{u}_{01}$ is the rigid body displacements.

Imposing compatibility of displacements in the contact area, it follows that

$$\tilde{u}_2 - \tilde{u}_1 = -\int_a^\infty \frac{\partial u_2}{\partial r}\,\mathrm{d}r - \int_0^a \frac{\partial u_1}{\partial r}\,\mathrm{d}r = -\int_a^\infty \varepsilon_{2r}\,\mathrm{d}r - \int_0^a \varepsilon_{1r}\,\mathrm{d}r, \tag{A.2}$$

where $a = R_2 \approx R_1$. By means of Hooke's constitutive law, the stress formulae (37) can be easily expressed in terms of strains to give, under plane stress assumption,

$$\begin{aligned}
\varepsilon_{1r} &= \frac{1}{E_1}\frac{Q}{a}\left[-(1+\nu_1)\int_{-\varepsilon}^{+\varepsilon} q(\psi)L_2\,\mathrm{d}\psi + 2\nu_1\int_{-\varepsilon}^{+\varepsilon} q(\psi)L_1\,\mathrm{d}\psi\right] + \frac{Q}{a}F_1(r)\cos\phi,\\
\varepsilon_{2r} &= \frac{1}{E_2}\frac{Q}{a}\left[(1+\nu_2)\int_{-\varepsilon}^{+\varepsilon}\left(\frac{\rho^2-1}{2\pi\rho^2} + L_2\right)q(\psi)\,\mathrm{d}\psi - 2\nu_2\int_{-\varepsilon}^{+\varepsilon}\left(\frac{1}{2\pi} + L_1\right)q(\psi)\,\mathrm{d}\psi\right]\\
&\quad + \frac{Q}{a}F_2(r)\cos\phi,
\end{aligned} \tag{A.3}$$

where the auxiliary functions $F_1(r)$ and $F_2(r)$ are defined as

$$\begin{aligned}
F_1(r) &= -\frac{1+\nu_1}{4\pi E_1}\left[1 - \nu_1 - (1-3\nu_1)\rho^2\right]\frac{1}{\rho},\\
F_2(r) &= \frac{3-\nu_2}{4\pi E_2}\left[1 - \nu_2 - (1+\nu_2)\frac{1}{\rho^2}\right]\frac{1}{\rho}.
\end{aligned} \tag{A.4}$$

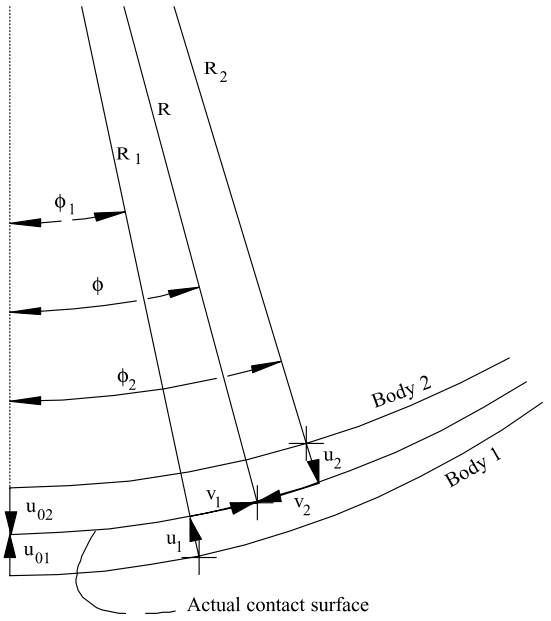

Fig. 10. Displacements at the contact region.

By substituting Eq. (A.3) into Eq. (A.2), and after performing somewhat lengthy calculations, the following integral equation for the contact pressure is derived

$$(1+\eta)\int_{-\varepsilon}^{+\varepsilon} q'(\psi)\cot\frac{(\psi-\phi)}{2}\,\mathrm{d}\psi + [2(1+\eta)-\lambda]\int_{-\varepsilon}^{+\varepsilon} q(\psi)\cos(\psi-\phi)\,\mathrm{d}\psi = -\lambda\pi q(\phi) - \eta\int_{-\varepsilon}^{+\varepsilon} q(\psi)\mathrm{d}\psi - \frac{\pi E_1 \Delta R}{Q} \tag{A.5}$$

with the equilibrium condition

$$\int_{-a}^{+a} q(\psi)\cos(\psi-\phi)\,\mathrm{d}\psi = \cos\phi. \tag{A.6}$$

After employing Eq. (5), Eqs. (3) and (4) of Section 2 are derived by rearranging the Eqs. (A.5) and (A.6).

References

Davis, P.F., Rabinowitz, P., 1984. Methods of Numerical Integration, second ed. Academic Press, London.

Dundurs, J., 1975. Properties of elastic bodies in contact. In: de Pater, A.D., Kalker, J.J., (Eds.), Mechanics of Contact Between Deformable Bodies. Delft University Press, Delft.

Dundurs, J., 1969. Discussion of edge-bonded dissimilar orthogonal elastic wedges under normal and shear loading. Journal of Applied Mechanics 36, 650–652.

Gladwell, G.M.L., 1980. Contact Problems in the Classical Theory of Elasticity, Sijthoff and Noordhoff, Alphen aan den Rijn.

Ghosh, S.P., Dattaguru, B., Rao, A.K., 1981. Load transfer from a smooth elastic pin to a large sheet. AIAA J. 19 (5), 619–625.

Hills, D.A., Nowell, D., Sackfield, A., 1993. Mechanics of Elastic Contacts. Butterworth-Heinemann, Oxford.

Johnson, K.L., 1985. Contact Mechanics. Cambridge University Press, Cambridge.

Lin, S., Hills, D.A., Nowell, D., 1997. Stresses in a flat plate due to a loose pin pressing against a cracked hole. Journal of Strain Analytical Engineering Design 32 (2), 145–156.

Hussain, N., 1969. Exact solution of certain dual series for indentation and inclusion problems. International Journal of Engineering Science 7, 1149–1161.

Persson, A., 1964. On the stress distribution of cylindrical elastic bodies in contact, Ph.D. dissertation, Chalmers, Tekniska, Goteborg, Sweden.

Shtaermann, I.Ya., 1949. Contact Problem of the Theory of Elasticity, Moscow, Leningrad: Gostekhteoretizdat. Available from the British Library in a English translation by Foreign Technology Div., FTD-MT-24-61-70, 1970.